Research Article | Vol. 25, No. 13 | 26 Jun 2017 | OPTICS EXPRESS 16059
Optics EXPRESS

Temperature-strain discrimination in distributed optical fiber sensing using phase-sensitive optical time-domain reflectometry

XIN LU,[1,*] MARCELO A. SOTO,[1] AND LUC THÉVENAZ[1,2]

[1]*EPFL Swiss Federal Institute of Technology, Institute of Electrical Engineering, SCI STI LT, Station 11, CH-1015 Lausanne, Switzerland*
[2]*luc.thevenaz@epfl.ch*
[*]*luxin1026@gmail.com*

Abstract: A method based on coherent Rayleigh scattering distinctly evaluating temperature and strain is proposed and experimentally demonstrated for distributed optical fiber sensing. Combining conventional phase-sensitive optical time-domain domain reflectometry (ϕOTDR) and ϕOTDR-based birefringence measurements, independent distributed temperature and strain profiles are obtained along a polarization-maintaining fiber. A theoretical analysis, supported by experimental data, indicates that the proposed system for temperature-strain discrimination is intrinsically better conditioned than an equivalent existing approach that combines classical Brillouin sensing with Brillouin dynamic gratings. This is due to the higher sensitivity of coherent Rayleigh scatting compared to Brillouin scattering, thus offering better performance and lower temperature-strain uncertainties in the discrimination. Compared to the Brillouin-based approach, the ϕOTDR-based system here proposed requires access to only one fiber-end, and a much simpler experimental layout. Experimental results validate the full discrimination of temperature and strain along a 100 m-long elliptical-core polarization-maintaining fiber with measurement uncertainties of ~40 mK and ~0.5 με, respectively. These values agree very well with the theoretically expected measurand resolutions.

OCIS codes: (060.2370) Fiber optics sensors; (120.4825) Optical time domain reflectometry; (260.1440) Birefringence; (290.5870) Scattering, Rayleigh.

References and links

1. J. P. Dakin, D. J. Pratt, G. W. Bibby, and J. N. Ross, "Distributed optical fibre Raman temperature sensor using a semiconductor light source and detector," Electron. Lett. **21**(13), 569–570 (1985).
2. T. Horiguchi, K. Shimizu, T. Kurashima, M. Tateda, and Y. Koyamada, "Development of a distributed sensing technique using Brillouin scattering," J. Lightwave Technol. **13**(7), 1296–1302 (1995).
3. Y. Koyamada, M. Imahama, K. Kubota, and K. Hogari, "Fiber-optic distributed strain and temperature sensing with very high measurand resolution over long range using coherent OTDR," J. Lightwave Technol. **27**(9), 1142–1146 (2009).
4. A. Motil, A. Bergman, and M. Tur, "State of the art of Brillouin fiber-optic distributed sensing," Opt. Laser Technol. **78**, 81–103 (2016).
5. M. A. Soto and L. Thévenaz, "Modeling and evaluating the performance of Brillouin distributed optical fiber sensors," Opt. Express **21**(25), 31347–31366 (2013).
6. M. Nikles, L. Thevenaz, and P. A. Robert, "Brillouin gain spectrum characterization in single-mode optical fibers," J. Lightwave Technol. **15**(10), 1842–1851 (1997).
7. M. E. Froggatt, D. K. Gifford, S. Kreger, M. Wolfe, and B. J. Soller, "Characterization of polarization-maintaining fiber using high-sensitivity optical-frequency-domain reflectometry," J. Lightwave Technol. **24**(11), 4149–4154 (2006).
8. X. Lu, M. A. Soto, and L. Thévenaz, "MilliKelvin resolution in cryogenic temperature distributed fibre sensing based on coherent Rayleigh scattering," Proc. SPIE **9157**, 91573R (2014).
9. M. N. Alahbabi, Y. T. Cho, and T. P. Newson, "Simultaneous temperature and strain measurement with combined spontaneous Raman and Brillouin scattering," Opt. Lett. **30**(11), 1276–1278 (2005).
10. G. Bolognini, M. A. Soto, and F. Di Pasquale, "Fiber-optic distributed sensor based on hybrid Raman and Brillouin scattering employing multi-wavelength Fabry-Pérot lasers," IEEE Photonics Technol. Lett. **21**(20), 1523–1525 (2009).

#293161 https://doi.org/10.1364/OE.25.016059
Journal © 2017 Received 19 Apr 2017; revised 19 Jun 2017; accepted 24 Jun 2017; published 28 Jun 2017

Optics EXPRESS

11. G. Bolognini and M. A. Soto, "Optical pulse coding in hybrid distributed sensing based on Raman and Brillouin scattering employing Fabry-Perot lasers," Opt. Express **18**(8), 8459–8465 (2010).
12. S. M. Maughan, H. Kee, and T. P. Newson, "Simultaneous distributed fibre temperature and strain sensor using microwave coherent detection of spontaneous Brillouin backscatter," Meas. Sci. Technol. **12**(7), 834–842 (2001).
13. W. Zou, Z. He, and K. Hotate, "Complete discrimination of strain and temperature using Brillouin frequency shift and birefringence in a polarization-maintaining fiber," Opt. Express **17**(3), 1248–1255 (2009).
14. K. Y. Song, W. Zou, Z. He, and K. Hotate, "All-optical dynamic grating generation based on Brillouin scattering in polarization-maintaining fiber," Opt. Lett. **33**(9), 926–928 (2008).
15. Y. Dong, L. Chen, and X. Bao, "Truly distributed birefringence measurement of polarization-maintaining fibers based on transient Brillouin grating," Opt. Lett. **35**(2), 193–195 (2010).
16. K. Y. Song, W. Zou, Z. He, and K. Hotate, "Optical time-domain measurement of Brillouin dynamic grating spectrum in a polarization-maintaining fiber," Opt. Lett. **34**(9), 1381–1383 (2009).
17. K. Y. Song, "High-sensitivity optical time-domain reflectometry based on Brillouin dynamic gratings in polarization maintaining fibers," Opt. Express **20**(25), 27377–27383 (2012).
18. Y. Dong, L. Teng, P. Tong, T. Jiang, H. Zhang, T. Zhu, L. Chen, X. Bao, and Z. Lu, "High-sensitivity distributed transverse load sensor with an elliptical-core fiber based on Brillouin dynamic gratings," Opt. Lett. **40**(21), 5003–5006 (2015).
19. L. Teng, H. Zhang, Y. Dong, D. Zhou, T. Jiang, W. Gao, Z. Lu, L. Chen, and X. Bao, "Temperature-compensated distributed hydrostatic pressure sensor with a thin-diameter polarization-maintaining photonic crystal fiber based on Brillouin dynamic gratings," Opt. Lett. **41**(18), 4413–4416 (2016).
20. Y. H. Kim, H. Kwon, J. Kim, and K. Y. Song, "Distributed measurement of hydrostatic pressure based on Brillouin dynamic grating in polarization maintaining fibers," Opt. Express **24**(19), 21399–21406 (2016).
21. M. A. Soto, X. Lu, H. F. Martins, M. Gonzalez-Herraez, and L. Thévenaz, "Distributed phase birefringence measurements based on polarization correlation in phase-sensitive optical time-domain reflectometers," Opt. Express **23**(19), 24923–24936 (2015).
22. H.-J. Yoon, D. M. Costantini, H. G. Limberger, R. P. Salathé, C.-G. Kim, and V. Michaud, "In situ strain and temperature monitoring of adaptive composite materials," J. Intell. Mater. Syst. Struct. **17**(12), 1059–1067 (2006).
23. A. D. Kersey, M. A. Davis, H. J. Patrick, M. LeBlanc, K. P. Koo, C. G. Askins, M. A. Putnam, and E. J. Friebele, "Fiber grating sensors," J. Lightwave Technol. **15**(8), 1442–1463 (1997).
24. J. R. Taylor, *An Introduction to Error Analysis* (University Science Books, 1997).
25. A. Zornoza, D. Olier, M. Sagues, and A. Loayssa, "Brillouin distributed sensor using RF shaping of pump pulses," Meas. Sci. Technol. **21**(9), 094021 (2010).
26. H. F. Martins, S. Martin-Lopez, P. Corredera, M. L. Filograno, O. Frazao, and M. González-Herráez, "Coherent noise reduction in high visibility phase-sensitive optical time domain reflectometer for distributed sensing of ultrasonic waves," J. Lightwave Technol. **31**(23), 3631–3637 (2013).
27. M. Ren, D. P. Zhou, L. Chen, and X. Bao, "Influence of finite extinction ratio on performance of phase-sensitive optical time-domain reflectometry," Opt. Express **24**(12), 13325–13333 (2016).
28. Y. H. Kim and K. Y. Song, "Characterization of nonlinear temperature dependence of Brillouin dynamic grating spectra in polarization-maintaining fibers," J. Lightwave Technol. **33**(23), 4922–4927 (2015).

1. Introduction

Distributed optical fiber sensors based on Rayleigh, Brillouin or Raman scattering have been the subject of research and development for several decades [1–3]. They enable a monitoring of environmental variables, such as temperature, strain or vibrations, continuously along an optical fiber. While each of these three types of distributed fiber sensor offers specific features and advantages in terms of performance, they also have very specific drawbacks. For instance, Raman distributed fiber sensors [1] offer the possibility to measure distributed temperature with no cross-sensitivity with other environmental variables, such as strain. However, since the system is based on the thermally-activated spontaneous Raman scattering, which is very weak in optical fibers, the sensing distance and measurand resolution (traded-off with the spatial resolution) turn out to be limited. In Brillouin distributed sensing [2], measurements are based on the acquisition of the local Brillouin gain/loss spectrum, from which the longitudinal Brillouin frequency profile is retrieved to provide a distributed map of the longitudinal temperature and strain information [4,5]. Whilst Brillouin sensors can inherently provide more accurate measurements and achieve longer distances than Raman sensors, they are typically affected by the cross-sensitivity of the Brillouin frequency on the temperature and strain [6]. On the other hand, distributed fiber sensors based on coherent Rayleigh scattering [3] utilize the restorability features of the temporal trace shape to measure temperature and strain, which

Optics EXPRESS

can be obtained by using techniques such as optical time-domain reflectometry (OTDR) [3] or optical frequency-domain reflectometry (OFDR) [7]. While OFDR can provide very sharp spatial resolution over a limited sensing range, the OTDR technique is usually more suitable for sensing over long distances, typically with metric spatial resolution. In coherent Rayleigh sensing, the optical fiber behaves similarly to a long, weak fiber Bragg grating (FBG) with random amplitude and pitch, which makes the coherent Rayleigh sensor as sensitive as a FBG sensor: this is three orders of magnitude more sensitive than a Brillouin sensor [8]. However, similarly to Brillouin and FBG sensors, coherent Rayleigh sensing systems are also affected by the temperature-strain cross-sensitivity. Furthermore, unlike other distributed fiber sensors, ϕOTDR sensors provide only measurements of relative temperature and strain changes, instead of absolute values. Being a highly sensitive sensor, the system typically requires a very broad spectral scanning range, thus increasing the complexity and cost of the sensor.

Temperature-strain cross-sensitivity is one of the main troublesome effects affecting the accuracy of high-performance distributed fiber sensing. In order to obtain independent strain and temperature profiles, an abundance of approaches has been proposed in the literature for many years, among which a much limited subset results in a non-ill-conditioned discrimination [9–19]. For instance by combining distributed measurements of the amplitude of the spontaneous anti-Stokes Raman scattering and the Brillouin frequency shift, temperature-strain discrimination has been demonstrated [9–11]. Another approach has been proposed to combine measurements of the spontaneous Brillouin scattering amplitude and Brillouin frequency shift [12]. In these two cases, the low power of the spontaneous scatterings (either Raman or Brillouin), as well as the low sensitivity of the spontaneous Brillouin scattering amplitude have basically constrained the accuracy on the discrimination. Another more recent technique [13] has been proposed by combining a Brillouin dynamic grating (BDG) [14] with classical Brillouin scattering. BDGs actually allow distributed measurements of the phase birefringence along polarization-maintaining (PM) fibers [14,15]. Due to the dependence of birefringence on environmental conditions, BDGs has been widely exploited to monitor variables such as temperature, strain, transverse load and hydrostatic pressure [16–20]. Thus, by combining BDG-based birefringence measurements and standard Brillouin sensing, temperature and strain can be robustly discriminated along a single optical fiber [13]. Using similar approaches distributed hydrostatic pressure has also been separated from temperature, as reported in Ref [19,20].

Besides the possibilities for temperature-strain discrimination, distributed fiber sensing based on birefringence measurements has also demonstrated very interesting features by itself. Thus, for instance, using BDGs the measured temperature and strain sensitivities of the fiber birefringence has demonstrated to be one order of magnitude higher than the sensitivities shown by classical Brillouin sensing techniques. This feature actually makes birefringence-based distributed sensing a very appealing approach for a wide range of applications. However, the writing and reading processes of Brillouin dynamic gratings usually make use of high-power optical signals and a complex system, requiring also access to both fiber-ends.

As an alternative, distributed measurements of the phase birefringence can also be obtained using coherent Rayleigh scattering inside the fiber, using either OFDR [7], or ϕOTDR [21]. In both approaches measurements of the coherent Rayleigh scattering are obtained along the two main orthogonal axes of polarization of a birefringent fiber. By cross-correlating their spectral responses, a correlation peak is obtained at a frequency shift proportional to fiber birefringence. Very accurate distributed birefringence profile can be obtained using this Rayleigh-based approach, which requires access only to one fiber end. Interestingly, not only high-birefringence fibers can be measured with this Rayleigh approach, but also low-birefringence single-mode fibers have been characterized using ϕOTDR [21].

In this paper, a method to discriminate temperature and strain in distributed fiber sensing is proposed and experimentally validated based on coherent Rayleigh scattering. First, the capability of a polarization-resolved ϕOTDR system for distributed temperature and strain

Optics EXPRESS

sensing based on birefringence measurements is experimentally demonstrated. Results verify that, contrarily to conventional ϕOTDR sensing (which provides measurements relative to a reference), ϕOTDR-based birefringence measurements provide the possibility to obtain distributed profiles of the absolute temperature and strain along the fiber. Although the birefringence-based temperature and strain sensitivities are lower than in a conventional ϕOTDR sensor, they are still one order of magnitude higher than classical distributed Brillouin sensing. This is indeed an important feature of the here proposed system, since for many practical applications ϕOTDR sensing is too sensitive (typically leading to extremely large frequency scanning ranges); and therefore, in this case, a large measurand range can be obtained using a reduced frequency scanning range. Moreover, combining ϕOTDR-based birefringence measurements and classical ϕOTDR sensing, temperature-strain discrimination over an elliptical-core PM fiber is experimentally demonstrated. The presented analysis and obtained results point out that proposed technique has relevant advantages over the similar approach based on combining BDG and classical Brillouin measurements [16]: while the system configuration is here much simpler than a BDG scheme (e.g. requiring only moderate optical power and access to only one fiber-end), the high sensitivity of coherent Rayleigh scattering can also enable a more accurate temperature-strain discrimination.

2. Working principle

2.1 Birefringence measurements based on coherent Rayleigh scattering

In a ϕOTDR system [3], an optical pulse from a coherent light source is launched along an optical fiber and a small portion of the incident light is backscattered due to the non-perfectly uniform fiber density (resulting in small refractive index variations). The light reflected from different scattering points within the pulse width interferes in the photodetector. The stochastic variations of the refractive index along the fiber lead to a random interference process, resulting in a time-domain trace showing a speckle-like shape. The longitudinal shape of the time-domain trace is determined by the longitudinal refractive index variations along the fiber, the scattering point size, and the optical frequency used for interrogation. If temperature or strain changes at a given position of the fiber, the local material density (refractive index and scattering point size) will change due to thermo-optic effect, thermal expansion or photo-elastic effect. The principle of the ϕOTDR sensor is based on measuring the optical path variations (induced by temperature and strain changes) by compensating locally-induced trace shape changes with a shift in the optical frequency of the incident light. As a result, the frequency shift that restores the original local shape of the time-domain trace is proportional to the local optical path change, which in turn is proportional to the local temperature/strain variation [3].

In order to accurately determine the frequency shift carrying the environmental information, the response of the interference process from coherent Rayleigh scattering is measured at each fiber position as a function of optical frequency of the interrogating pulses [3,21]. The spectral response measured at a given fiber location exhibits an irregular shape, as shown in Fig. 1(a), due to the random interference process. Figure 1(a) points out that, when temperature changes, the local spectral response of the ϕOTDR measurements shifts with a sensitivity equal to a FBG sensor (e.g. in the figure, a temperature change of −26 mK induces a spectral shift of 30 MHz). Similar behavior can be observed if strain changes locally in the sensing fiber. Consequently, the environmental variations can be obtained from the frequency shift of the Rayleigh backscattered spectrum. Considering that the spectral response has an irregular shape, a reliable method to determine the frequency shift is to cross-correlate the spectrum measured at a given position and time, with a reference spectrum measured during a calibration stage under known environmental conditions. Figure 1(b) illustrates the cross-correlation of the spectra in Fig. 1(a), showing a correlation peak around 30 MHz. Then, the correlation peak frequency can be precisely determined by fitting (e.g. with a quadratic curve) the local cross-correlation spectrum [5,8]. Finally, the temperature or strain change can be

Optics EXPRESS

related to the cross-correlation spectral shift using pre-calibrated temperature and strain sensitivities.

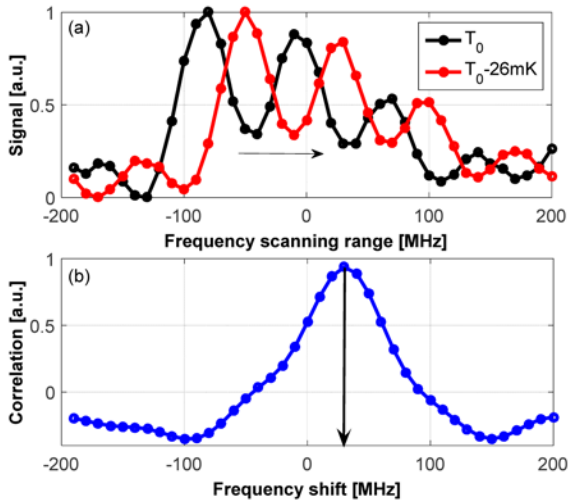

Fig. 1. (a) Reflection spectrum of the coherent Rayleigh light at a given position, showing the spectral shift due to the temperature change; (b) cross-correlation curve of the two reflection spectra.

In practice, the measurement process first requires to obtain a reference reflection spectrum $R_r(z, f)$ of the Rayleigh traces along the fiber within a defined frequency range. Then real-time measurements of the spectrum $R_t(z, f)$ are obtained at time t and compared with the reference measurement [3,21]. If there is no environmental perturbations between the two measurements, the cross-correlation peak of $R_r(z, f)$ and $R_t(z, f)$ is located at zero frequency shift; otherwise, a frequency shift Δf, proportional to the temperature or strain variation, is obtained. It has to be noted that this technique only provides a measurement of the relative temperature-strain change (with respect to the time when the reference traces were measured), instead of the absolute value.

Since the temporal traces measured by a ϕOTDR sensor depend on refractive index changes, the time-domain traces of the coherent Rayleigh scattering measured along the eigen axes of a PM fiber should have different shapes. Based on the same working principle explained before for a classical ϕOTDR sensor, the phase birefringence Δn can be retrieved along a PM fiber by cross-correlating the coherent Rayleigh traces measured along eigen axes of the fiber [21]. Thus, according to the phase matching condition, the local cross-correlation frequency shift measured with a polarization-resolved ϕOTDR system is proportional to the local birefringence [21]:

$$n_x(f_x) f_x = n_y(f_y) f_y \quad \rightarrow \quad \Delta f = \frac{-f_y}{n_y^g} \Delta n, \tag{1}$$

where f_x, f_y and n_x, n_y are the frequencies and refractive indices along the two orthogonal polarization axes (slow and fast axes), and n^g_y is the group refractive index of the fast axis. The typical birefringence for a PM fiber is around 4×10^{-4}, leading to a frequency shift of ~50 GHz. A fully detailed description about this polarization-resolved ϕOTDR method for distributed birefringence measurements can be found in Ref [21].

Optics EXPRESS

2.2 Temperature-strain discrimination

Birefringence is usually caused by the asymmetry of the fiber cross-section, which may be induced during the fiber fabrication and installation processes. In the case of PM fibers, an asymmetric stress or asymmetric doping is intentionally introduced into the fibers, so that light coupling between orthogonally polarized modes becomes difficult. Interestingly, the impact of the fiber asymmetry is highly dependent on environmental variables, such as temperature, strain or hydrostatic pressure. Therefore, fiber birefringence measurements can be exploited to measure local environmental conditions, like demonstrated using BDGs [16–20]. Unfortunately, this approach is also affected by cross-sensitivity issues (between temperature, strain and pressure).

The technique proposed in this paper exploits the dual potential functionality of a ϕOTDR system: on the one hand, a ϕOTDR system can be used to measure the coherent Rayleigh scattering along the two orthogonal polarization axes of the fiber, thus enabling distributed birefringence measurements [21]. On the other hand, the same system can be used for classical ϕOTDR sensing [3] based in the cross-correlation of coherent Rayleigh traces obtained from a given (same) polarization axis. In this way, by measuring two variables (i.e. local birefringence and local ϕOTDR frequency shift), independent temperature and strain profiles can be retrieved along the sensing fiber.

In practice, the birefringence-induced frequency shift Δf_{bire} can be obtained by cross-correlating coherent Rayleigh traces from orthogonal axes in a single measurement, while $\Delta f_{\phi OTDR}$ can be retrieved based on the cross-correlation of ϕOTDR traces from the same axis between two consecutive measurements. Considering that Δf_{bire} and $\Delta f_{\phi OTDR}$ depend on both temperature and strain variations, the system can be described as follows [13]:

$$\begin{bmatrix} \Delta f_{\phi OTDR} \\ \Delta f_{bire} \end{bmatrix} = \begin{bmatrix} S_{T,\phi OTDR} & S_{\varepsilon,\phi OTDR} \\ S_{T,bire} & S_{\varepsilon,bire} \end{bmatrix} \begin{bmatrix} \Delta T \\ \Delta \varepsilon \end{bmatrix}, \tag{2}$$

where ΔT and $\Delta\varepsilon$ are the temperature and strain changes, $S_{T,\phi OTDR}$ and $S_{\varepsilon,\phi OTDR}$ are the temperature and strain sensitivities of the classical ϕOTDR sensor, $S_{T,bire}$ and $S_{\varepsilon,bire}$ are the temperature and strain sensitivities of the fiber birefringence, $\Delta f_{\phi OTDR}$ and Δf_{bire} are correlation spectral shifts of the ϕOTDR sensor and the birefringence measurement, respectively. Inverting Eq. (2), and using the measured $\Delta f_{\phi OTDR}$ and Δf_{bire}, independent temperature and strain profiles can be retrieved [13]:

$$\begin{bmatrix} \Delta T \\ \Delta \varepsilon \end{bmatrix} = \frac{1}{S_{T,\phi OTDR} S_{\varepsilon,bire} - S_{\varepsilon,\phi OTDR} S_{T,bire}} \begin{bmatrix} S_{\varepsilon,bire} & -S_{\varepsilon,\phi OTDR} \\ -S_{T,bire} & S_{T,\phi OTDR} \end{bmatrix} \begin{bmatrix} \Delta f_{\phi OTDR} \\ \Delta f_{bire} \end{bmatrix}. \tag{3}$$

In order to achieve reliable and precise temperature-strain discrimination, the matrix of coefficients S in Eq. (2) must be well-conditioned. This is typically evaluated by the so-called *condition number*, defined as $C(S) = \|S\|\|S^{-1}\|$, being $\|S\|$ the norm of the matrix S containing the coefficients of sensitivities. In order to reduce the uncertainties in the discrimination, a small conditional number is desired [22]. Considering that the temperature and strain sensitivities of a ϕOTDR system are, in principle, similar to the ones of FBGs (i.e. $S_{T,\phi OTDR} \approx$-1.3 GHz/K, $S_{\varepsilon,\phi OTDR} \approx$-150 MHz/με [23]) and the sensitivities of the fiber birefringence are $S_{T,bire}$ = –55.8 MHz/K and $S_{\varepsilon,bire}$ = 0.8995 MHz/με (according to BDG-based measurements [13]), then the condition number of the here proposed technique is expected to be ~179.8. This value is much smaller than the conditional number (~989.4) obtained by the similar approach using Brillouin sensing combined with BDG measurements [13]. Thus, the matrices in Eqs. (2) and (3) are better conditioned using coherent Rayleigh scattering, which can be explained

basically by high sensitivities of the ϕOTDR measurements when compared to Brillouin sensing methods.

From Eq. (3), the error in the discriminated temperature $\sigma_{\Delta T}$ and strain $\sigma_{\Delta\varepsilon}$ can be obtained as [24]:

$$\sigma_{\Delta T} = \frac{\sqrt{\left(S_{\varepsilon,bire}\cdot\sigma_{\Delta f,\phi OTDR}\right)^2+\left(S_{\varepsilon,\phi OTDR}\cdot\sigma_{\Delta f,bire}\right)^2}}{\left|S_{T,\phi OTDR}S_{\varepsilon,bire}-S_{\varepsilon,\phi OTDR}S_{T,bire}\right|}, \tag{4}$$

$$\sigma_{\Delta\varepsilon} = \frac{\sqrt{\left(S_{T,bire}\cdot\sigma_{\Delta f,\phi OTDR}\right)^2+\left(S_{T,\phi OTDR}\cdot\sigma_{\Delta f,bire}\right)^2}}{\left|S_{T,\phi OTDR}S_{\varepsilon,bire}-S_{\varepsilon,\phi OTDR}S_{T,bire}\right|}, \tag{5}$$

where $\sigma_{\Delta f,\phi OTDR}$ and $\sigma_{\Delta f,bire}$ represent the standard deviation of the frequency shift obtained by the classical ϕOTDR measurements and the ϕOTDR-based birefringence measurements, respectively. Note that Eqs. (4)-(5) can also be applied to analyze errors resulting from using OFDR sensing, which basically exhibits the same sensitivity as the ϕOTDR technique.

3. Experimental setup

The experimental setup here used for temperature-strain discrimination is based on the birefringence measurement system described in Ref [21]. The configuration shown in such a reference is however not optimized for sensing, since the high sensitivity of the ϕOTDR technique can eventually introduce large measurement errors due to the potential environmental perturbations changing during the acquisition process. To improve the reliability of the measurements, the traces from the two orthogonal axes of the PM fiber must be acquired simultaneously to avoid any detrimental perturbations (e.g. temperature fluctuations) between the two polarization measurements. A potential simple alternative is to measure the coherent Rayleigh scattering from the two polarization axes in a very small time-scale, so that eventual temperature or strain variations could be ignored during this measurement time interval.

Figure 2 shows the experimental setup used for measuring the coherent Rayleigh time-domain traces along two orthogonal axes of a PM fiber, within a time interval of a few microseconds. In this case, two semiconductor lasers operating at a wavelength around 1534 nm are employed for the measurement of the fast and slow axes, respectively. The use of two lasers enables to scan independent frequency ranges along the two axis of polarization, thus avoiding an unnecessarily wide spectral scanning range. This way, the optical frequency difference between the two lasers has been set to coarsely match the birefringence of the PM fiber by tuning the driving current of the lasers. A fine frequency scanning is then performed by intensity modulation, as described hereafter. As detailed in Ref. 21, this approach enables a precise scanning of the spectral cross-correlation peak while addressing a reduced number of scanned frequencies. Firstly, the continuous lightwaves from the two lasers are coupled and split using a 2 × 2 optical coupler. Part of the combined light is launched into an optical spectrum analyzer (OSA) with 5 MHz resolution to monitor the optical frequency difference of the lasers. The other fraction of the light passes through an electro-optic modulator (EOM) driven by a radio-frequency (RF) pulse to generate an optical pulse with tunable frequency. The optical pulses generated with this RF method exhibit an extremely high extinction ratio (up to 60 dB) [25], which is crucial to reduce the coherent noise in the measurements potentially induced by a DC leak component [26,27]. Then two narrow band FBGs are used (~7 GHz FWHM), each of them is properly tuned to select one sideband from each laser after modulation. One of the selected sidebands is launched into an optical delay line in order to temporarily offset the two optical pulses at different frequencies. To avoid the overlapping of the Rayleigh traces from different axes, the applied relative delay has to be longer than the

Optics EXPRESS

round-trip time-of-flight along the sensing PM fiber. In this case, a short optical fiber of 680 m is used, thus providing a delay of 3.4 μs and allowing for a sensing range of up to 340 m. Then, the polarization of the optical pulses is adjusted by polarization controllers (PCs) so that the pulses at different frequencies are then coupled with orthogonal polarizations using a polarization beam combiner. The optical pulses are amplified by an erbium-doped fiber amplifier (EDFA) and an optical bandpass filter is employed to suppress the amplified spontaneous emission (ASE) from the EDFA. A third PC is used to align the orthogonally-polarized pulses to the corresponding axes of the PM fiber. Coherent Rayleigh scattering traces are measured by a 125 MHz photodetector, connected to a computer for data acquisition.

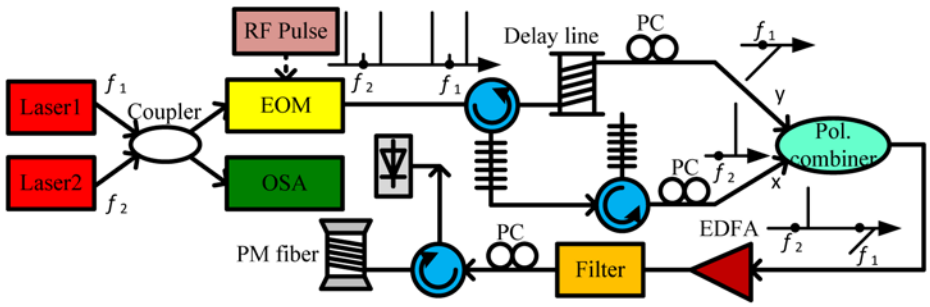

Fig. 2. Experimental setup to acquire the Rayleigh traces from 2 orthogonal axes in a very short time scale (milliseconds).

A 100 m-long elliptical-core PM fibers is used to validate the here proposed technique for temperature-strain discrimination. The pulse width is set to 20 ns, corresponding to 2 m spatial resolution. The Rayleigh traces are measured by scanning the pulse optical frequency in a range of 2 GHz with 5 MHz step. To reduce the impact of detection noise, traces are averaged 500 times, leading to a whole measurement time of ~1 min (for the 400 scanned frequencies). Note that the spectral measurements using the OSA have confirmed that the frequency stability of the two lasers remains below the OSA resolution of 5 MHz within the measurement time, thus having a minimum impact on the precision of the birefringence measurements.

4. Experimental results and discussion

4.1 Distributed birefringence measurements

Based on previous measurements, this fiber has an average birefringence of 3×10^{-4}, which corresponds to an average frequency shift of ~43.1 GHz [21]. By tuning the optical frequency of the two lasers to such a frequency difference, coherent Rayleigh scattering traces have been sequentially acquired from the two polarization axes of the PM fiber with a time difference of 3.4 μs. The sequential Rayleigh traces from orthogonal fiber axes are shown in Fig. 3(a), where the first trace corresponds to the coherent Rayleigh pattern measured along the slow axis, and the second trace (delayed by 3.4 μs) is the backscattering measured along the fast axis. It should be noted that the delay between traces can be considered sufficiently small, so that changes in the environmental conditions (e.g. temperature changes) can be fully ignored during the acquisition of the traces along the two orthogonal axes.

Optics EXPRESS

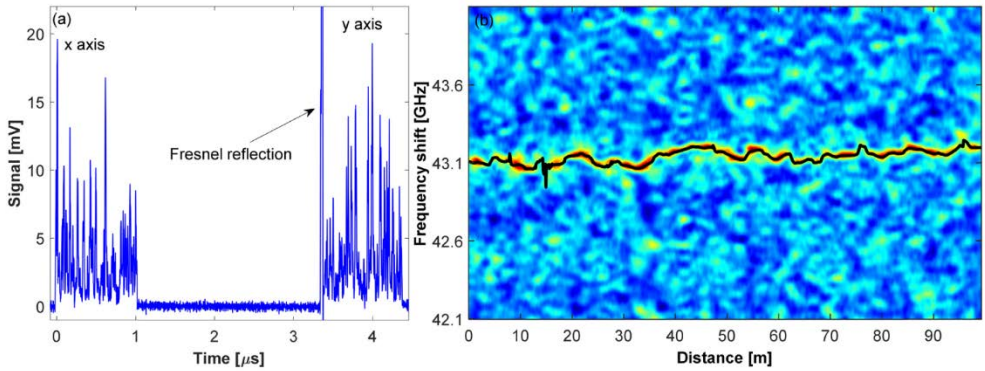

Fig. 3. Birefringence measurement of an elliptical-core PM fiber. (a) Time-shifted Rayleigh traces obtained for both polarization axes and (b) cross-correlation of the Rayleigh traces.

After scanning a frequency range of 2 GHz, the spectral cross-correlation of the Rayleigh traces from the two axes is calculated at each fiber position, as illustrated in Fig. 3(b). The figure shows a top view of the cross-correlation spectrum, along with the actual frequency shift profile determined by the local fiber birefringence (black line). This distributed profile has been obtained by fitting the correlation peak spectrum with a quadratic curve at each fiber position [5,8]. Thus, using Eq. (1) and the measured frequency shift profile, the local birefringence Δn can be calculated.

4.2 Distributed temperature and strain sensing based on birefringence

Since birefringence is dependent on the environmental variations, the proposed technique based on coherent Rayleigh scattering is first validated for distributed temperature and strain sensing. Temperature and strain are independently applied along the last ~3.5 m of fiber. Firstly, the temperature of the last few meters of the fiber has been changed in a range of ~13°C by placing the fiber section inside a thermal bath with a temperature control accuracy of 0.1 K. Then, strain variations of up to ~640 με are induced by attaching a short section (2 m) of the optical fiber to a precise moving stage (no temperature change is applied in this case).

Figure 4 shows the measured distributed profile of the birefringence-induced frequency shift at the end of the elliptical-core fiber under different temperature and strain conditions. Results demonstrate the ability of the system to measure birefringence changes induced by temperature and strain variations. It is interesting to notice that when temperature changes are applied to the fiber (see Fig. 4(a)), the rest of the fiber also shows small birefringence changes. This is presumably due to heat propagation through the fiber or air, from the hot-spot section to neighboring regions. It should be mentioned that for a precise characterization of the birefringence response as a function of the applied temperature, traces are measured after a long temperature stabilization time. This procedure enables precise temperature characterization, however, gives enough time for the heat to propagate to neighboring regions, and affect the birefringence measurements, as shown in Fig. 3(a). On the other hand, strain measurements do not need additional time for stabilization, so the impact of the environmental perturbations is, in this case, minimized. Figure 4(b) shows the measured frequency shift induced by strain, applying up to ~640 με. Frequency fluctuations as low as ± 3 MHz could be observed in the non-strained section (given essentially due to thermal fluctuations in the order of a few mK).

Optics EXPRESS

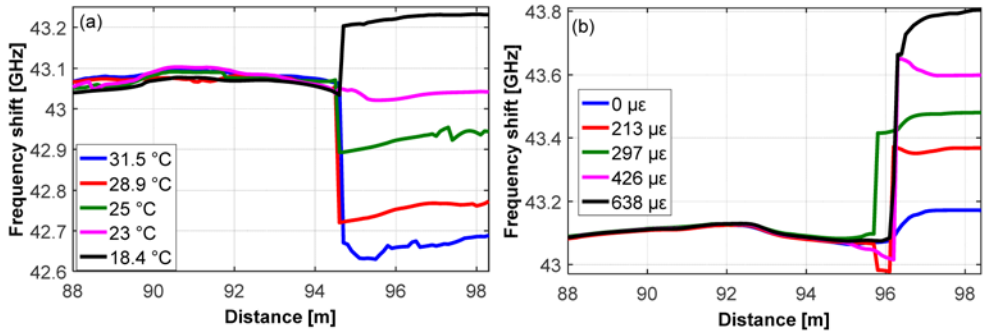

Fig. 4. Birefringence-dependent frequency shift measured versus distance (along the last 10 m of fiber) with a polarization-resolved ϕOTDR under different (a) temperature and (b) strain conditions for an elliptical-core PM fiber.

To evaluate the temperature and strain sensitivity of the fiber birefringence, the average value of the measured frequency shifts in Fig. 4 (within the perturbed zones) are considered for each applied temperature and strain. Results show a linear dependence of the birefringence on the temperature (Fig. 5(a)) and strain (Fig. 5(b)), while the slopes represent the corresponding sensitivities. The temperature and strain sensitivities of the birefringence are about −44 MHz/K and ~1 MHz/με, respectively, corresponding to over 40 times and 20 times higher than the respective sensitivities shown by Brillouin scattering. However, attention must be paid to the potential nonlinear temperature dependence of the fiber birefringence over an extended temperature range [28]. Thus, in order to measure large temperature changes, a thorough calibration might be required to apply the method proposed in this paper.

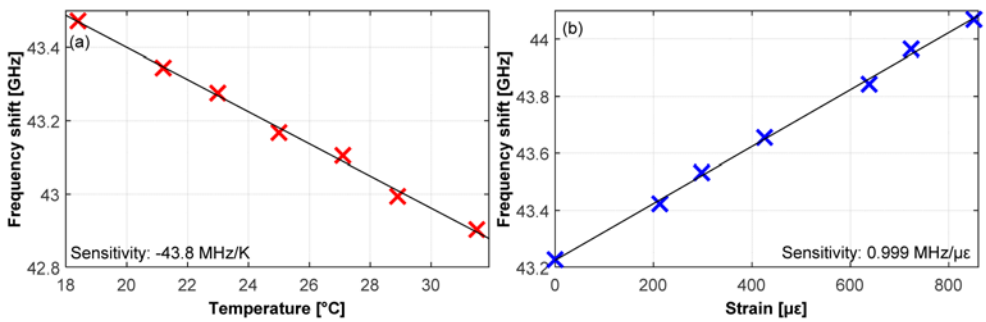

Fig. 5. Birefringence-dependent frequency shift measured with a polarization-resolved ϕOTDR as a function of (a) temperature and (b) strain for an elliptical-core PM fiber.

4.3 Discrimination of temperature and strain

To demonstrate the discrimination of temperature and strain, birefringence measurements based on the experimental setup shown in Fig. 2 have been consecutively obtained using the previously characterized elliptical-core fiber. Before the actual measurement, the temperature and strain sensitivities of the ϕOTDR measurements have also been characterized along the slow axis of the elliptical-core PM fiber using the same setup. Figure 6 presents the measured spectral shift of the ϕOTDR cross-correlation peak under different temperature and strain values, indicating that the sensitivities of coherent Rayleigh scattering, for this elliptical-core PM fiber, are −1.739 GHz/K and −149.5 MHz/με, respectively. Even though the measured stain sensitivity is very close to that of a FBG sensor, the temperature sensitivity is substantially higher than expected, which may be explained by the special structure and coating of the elliptical-core fiber.

Optics EXPRESS

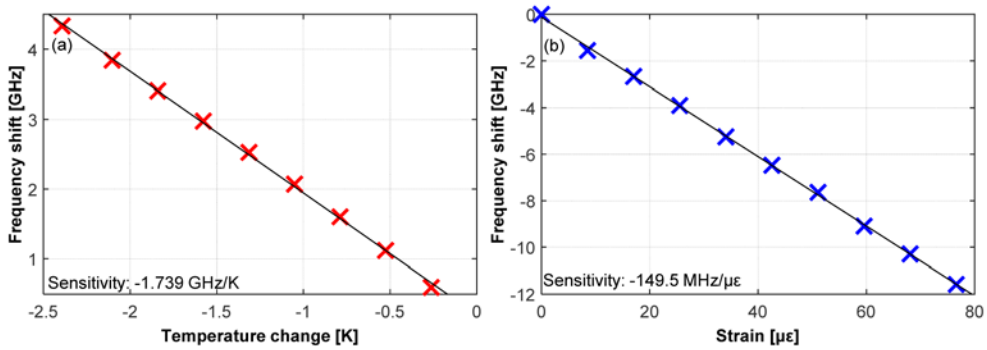

Fig. 6. Frequency shift of the cross-correlation spectrum measured using the ϕOTDR method, as a function of (a) temperature and (b) strain, for an elliptical core PM fiber.

Note that making use of the sensitivity coefficients measured here above (i.e. for both ϕOTDR and birefringence), a condition number equal to 376.9 is here obtained. This value is 2.7 times smaller than the condition number obtained when using classical Brillouin and BDG (~989.4) for temperature-strain discrimination [13]. This indicates that the ϕOTDR-based system here proposed is better conditioned than the Brillouin-based approach, due to the higher sensitivity of the coherent Rayleigh scattering, thus leading to smaller temperature-strain errors in the discrimination. However, the obtained condition number is higher than the theoretical prediction, probably as a direct consequence of the smaller actual values for $S_{T,bire}$ and $S_{\varepsilon,bire}$ in the tested PM fiber, which turn out to be directly scaled by the amount of birefringence. The elliptical core fiber has a smaller birefringence than the Panda fiber used for the theoretical estimation and the lower sensitivity of the birefringence on temperature and strain shows a dominating impact on the condition number.

In order to validate the here proposed technique to separate the distributed temperature and strain profiles, a temperature variation of 1.9 K and a strain change of 25.5 με are simultaneously applied at the end of the 100 m-long PM fiber between the two measurements (the first one representing the reference and the second the actual measurement). While, the full frequency scanning range is set to 9 GHz, with a 10 MHz frequency step, the environmental changes are chosen to be very small in order to probe the limit of this method and to demonstrate the high accuracy of the Rayleigh-based technique.

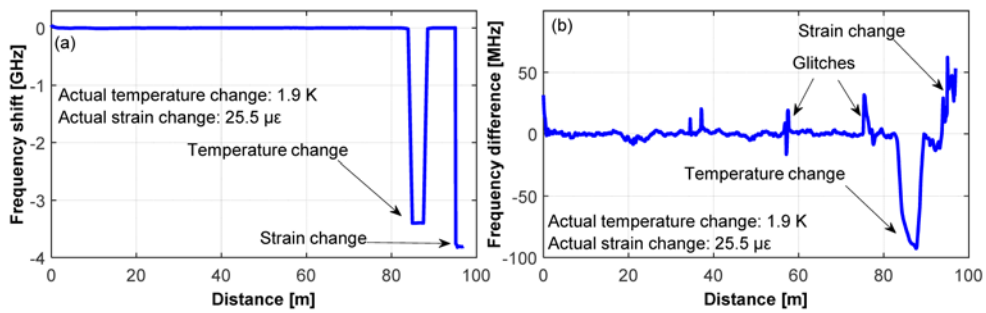

Fig. 7. (a) Frequency shift obtained from a standard ϕOTDR sensor and (b) frequency difference of birefringence measurements for an elliptical core PM fiber.

The cross-correlation of the coherent Rayleigh traces from slow axis obtained by two consecutive measurements provides the frequency shift of the standard ϕOTDR sensor, as shown in Fig. 7(a). Due to the large number of scanned frequencies (900 steps), a high-amplitude correlated peak is obtained, thus leading to a very clean frequency shift profile along the fiber. Because of this high-contrast correlation peak and the high sensitivities of the ϕOTDR

Optics EXPRESS

measurements, two very sharp frequency changes can be observed at the heated and strained fiber sections. On the other hand, the birefringence profile is obtained by cross-correlating the traces from orthogonal polarization axes. Figure 7(b) shows the frequency difference between two birefringence measurements, representing longitudinal variations of the fiber birefringence due to the environmental changes. The main limitation of this measurement is the random birefringence fluctuations occurring along the fiber, which reduce the amplitude and broaden the spectrum of the correlation peak obtained by cross-correlation. Due to the low-contrast correlation peak and the lower temperature and strain sensitivities, birefringence measurements are more vulnerable to noise, as can be observed in Fig. 7(b). This figure shows that the obtained frequency profile is noisier that the measured ϕOTDR-based frequency shift profile, and has some glitches that appear due to fast longitudinal variations of the local fiber birefringence (faster than the spatial resolution of 2 m). Fast longitudinal birefringence variations actually lead to a local broadening of the cross-correlation spectrum, making the detection of the correlation peak frequency more difficult. Thus, the fitting algorithm used in this case to obtain the peak frequency has led to glitches at positions where birefringence quickly changes along fiber sections shorter than the spatial resolution. This is a purely numerical issue in the fitting algorithm, thus indicating that a more robust and dedicated data processing method might be used to better determine the correlation peak frequency at those critical positions.

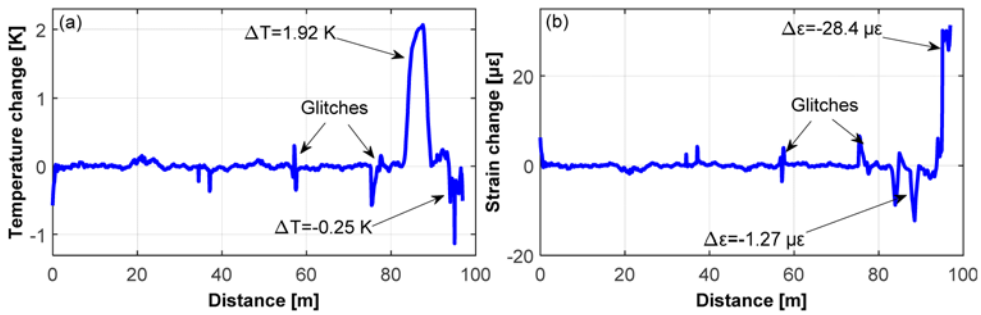

Fig. 8. Retrieved (a) temperature and (b) strain variation profiles along the elliptical core fiber. Results demonstrate that the ϕOTDR-based approach here proposed allows for a correct discrimination between distributed temperature and strain profiles.

Based on the frequency profile shown in Fig. 7, the temperature and strain distribution along the fiber are retrieved using Eq. (3). The two independent longitudinal profiles representing the temperature and strain changes along the fiber are shown in Fig. 8(a) and 8(b), respectively. Results demonstrate that temperature and strain can be discriminated by this Rayleigh-based technique, while the mean value of the measured temperature and strain changes (1.9 K and 28.4 με) agree very well with the applied values. A small cross-sensitivity is still observed in the retrieved profiles: a temperature change of −0.25 K is observed in the temperature profile around the strained section, while a strain variation of −1.3 με can be seen in the strain profile around the heated fiber region. These residual values are basically caused by the lower precision of the birefringence measurement, especially in regions where temperature or strain abruptly changes. These sharp environmental changes actually produce sharp variations of the local birefringence (along fiber sections shorter than the spatial resolution), thus inducing a significant broadening in the obtained correlation peak. This leads to a smoother birefringence profile, thus resulting in the residual temperature and strain observed in Fig. 8.

Considering the sensitivity coefficients obtained for both ϕOTDR and birefringence measurements, Eqs. (4)-(5) indicate that due to the lower sensitivity of the fiber birefringence, errors in the temperature-strain discrimination are essentially dominated by the uncertainty on

Optics EXPRESS

birefringence measurements. This is experimentally observed in Fig. 8, since both temperature and strain profiles contain the uncertainties (noise, and glitches) obtained in the birefringence measurement. Following a statistical approach based on calculating the standard deviation of the measurements at each fiber position, the frequency uncertainty in the classical ϕOTDR ($\sigma_{\Delta f,\phi OTDR}$) and ϕOTDR-based birefringence ($\sigma_{\Delta f,bire}$) measurements are 2.95 MHz and 2.19 MHz, respectively. Using these values in Eqs. (4)-(5), the errors in the temperature and strain estimation are calculated to be $\sigma_{\Delta T} \approx 39.5$ mK and $\sigma_{\Delta \varepsilon} \approx 0.459$ με. These values match very well the experimental temperature and strain uncertainties of ~40 mK and ~0.5 με, observed directly on the final temperature and strain profiles.

5. Conclusion

In this paper, a method to discriminate temperature and strain in distributed fiber sensing has been proposed and experimentally validated using an approach fully based on coherent Rayleigh scattering. Furthermore, distributed temperature and strain sensing using ϕOTDR-based birefringence measurements has also been demonstrated. The birefringence-based sensing using ϕOTDR demonstrates several advantages over existing distributed sensing techniques. It offers an intermediate sensitivity between Brillouin sensing methods and coherent Rayleigh based sensors, enabling a more accurate measurement (compared to Brillouin sensors) with a smaller frequency scanning range (compared to classical ϕOTDR sensors). Since the amount of birefringence primarily scales the sensitivity to temperature and strain and since the birefringence is artificially created by the fiber design, it offers a degree of freedom in the sensitivity scaling by targeting a proper value for birefringence. In addition, the proposed method requires a simpler experimental configuration compared to a BDG setup: lower optical powers and access to a single fiber end. Due to the high sensitivities shown by coherent Rayleigh scattering, this system discriminating temperature and strain turns out to be better conditioned that the equivalent approach based on BDG and Brillouin sensing, thus leading to smaller temperature and strain errors in this case. However, this high sensitivity imposes actual limitations to the maximum temperature and strain variations that can be measured, which are simply determined by the maximum frequency scanning range that can be implemented in the system. This is actually not a fundamental limitation of the ϕOTDR technique, but only practical.

The main limitation of the system lies on the ability to measure sharp longitudinal variations of the fiber birefringence (naturally present in the fiber or induced by abrupt temperature and strain changes). Thus, when the fiber birefringence varies longitudinally faster than the spatial resolution of the system, a weaker and broaden cross-correlation peak is locally obtained, making it more difficult to determine precisely the local correlation peak frequency. Those fast longitudinal variations of the fiber birefringence could, in principle, be better measured employing sharper spatial resolutions, however this would induce a spectral broadening of the correlation peak, thus restricting the smallest detectable birefringence change. Therefore, the trade-off between frequency uncertainty in the birefringence measurement and spatial resolution has to be suitably addressed in the system design.

Funding

Swiss Commission for Technology and Innovation (Project 18337.2 PFNM-NM).